

•装配式乡村住宅•

DOI:10.12454/j.jsuese.202500050



本刊网刊

套筒灌浆缺陷对装配式剪力墙抗震性能的影响

郑巍,张士前,马明磊,阴光华,陈少军

(中国建筑第八工程局有限公司,上海 200122)

摘要:为研究套筒灌浆缺陷对装配式混凝土剪力墙抗震性能的影响,以灌浆缺陷套筒数量、上侧钢筋灌浆缺陷长度为变化参数,设计7个钢筋套筒灌浆连接的装配式混凝土剪力墙(6个灌浆缺陷试件和1个灌浆饱满对比试件),完成拟静力试验,观察试件受力破坏过程和最终破坏形态,获取荷载-位移滞回曲线,分析试件滞回性能、骨架曲线、承载力、变形、刚度退化、延性和耗能能力等抗震性能指标。结果表明:套筒灌浆缺陷装配式混凝土剪力墙与灌浆饱满试件的破坏形态相似,最终破坏形态表现为边缘构件最外侧竖向钢筋受拉屈服甚至因套筒倾斜而拉断,且墙角套筒外侧混凝土保护层压碎脱落;灌浆缺陷试件的荷载-位移滞回曲线呈弓形或反“S”形;与灌浆饱满试件相比,套筒灌浆缺陷试件的承载力、变形和耗能能力减小,而灌浆缺陷对试件初始刚度影响不明显,但对后期刚度的影响逐渐变大;试件承载力、峰值位移和耗能能力随着灌浆缺陷套筒数量增加而减小,试件刚度随着灌浆缺陷套筒数量和套筒内灌浆缺陷长度增加而减小。

关键词:装配式剪力墙;套筒灌浆连接;灌浆缺陷;抗震性能;拟静力试验

中图分类号: TU375

文献标志码: A

文章编号: 2096-3246(2025)05-0052-12

装配式混凝土结构是中国建筑结构发展的重要方向之一,有利于中国建筑工业化的发展,具有提高生产效率、节约能源和绿色环保等显著优势^[1-3]。目前,装配式混凝土剪力墙结构在高层住宅建筑中应用广泛,对推进住宅产业化具有重要意义^[4-5]。装配式混凝土剪力墙竖向连接的可靠性对保证该结构体系受力性能至关重要。李然^[6]、朱张峰^[7]、Tang^[8]等对不同竖向连接构造的装配式混凝土剪力墙抗震性能进行了研究,研究结果表明,经合理设计的装配式混凝土剪力墙具有良好的整体性能,其抗震性能指标与现浇结构基本相同,满足在抗震设防区推广应用的要求。套筒灌浆连接技术可实现钢筋的可靠连接,是目前装配式混凝土结构中实现钢筋等强连接的主要连接技术之一^[9-12]。

国内外学者对套筒灌浆连接进行了大量试验及理论研究:Seo等^[13]开展灌浆套筒黏结性能试验,提出了灌浆套筒受拉强度计算方法;Henin等^[14]分析灌浆套筒传力机理,提出了套筒钢筋锚固长度计算方法;

Ling等^[15-16]采用锥形套筒开展钢筋锚固性能试验,研究表明,锥形套筒能有效利用套管壁的强度来增强黏结作用,提高锚固强度;余琼等^[17]对带肋钢筋与套筒约束灌浆料黏结性能进行试验研究,分析了钢筋与套筒约束灌浆料间黏结滑移本构关系,结果表明,由于套筒的约束,灌浆料与钢筋的锚固长度大大减小;许成顺等^[18]对高应力反复拉压作用下钢筋套筒灌浆连接性能进行试验研究,分析了钢筋与套筒约束灌浆料间黏结滑移本构关系;郑永峰等^[19]研究了套筒内腔构造对钢筋套筒灌浆连接黏结性能的影响,结果表明,增加套筒环肋数量及内壁凸起高度,可提高钢筋套筒灌浆连接的承载力;李锐等^[20]对钢筋套筒灌浆连接预制柱抗震性能进行了试验研究,结果表明,预制柱的位移延性、耗能能力和承载力均与现浇柱相近;余琼等^[21]对钢筋套筒灌浆搭接连接的预制剪力墙进行了抗震试验研究,结果表明,套筒在预制混凝土剪力墙中能够很好地传递钢筋应力,预制墙极限承载力与现浇墙基本相同;马军卫等^[22]开展了全装配式钢筋混凝

收稿日期:2025-01-22 修回日期:2025-03-11 网络出版日期:2025-03-11

基金项目:国家重点研发计划项目(2022YFC3801400;22dz1203104)

作者简介:郑巍(1990—),男,工程师。研究方向:装配式混凝土结构。E-mail: tumuzhengwei@163.com

土框架-剪力墙结构抗震性能试验研究,结果表明,灌浆套筒可有效传递钢筋应力;刘洪涛等^[23]对钢筋混凝土框架梁柱节点灌浆套筒连接抗震性能进行了研究,结果表明,预制装配梁柱节点试件的耗能能力略低于现浇整体梁柱节点试件的耗能能力;钱稼茹等^[24]对钢筋套筒灌浆连接装配式剪力墙结构3层足尺模型子结构进行了拟动力试验研究,结果表明,装配式结构“强墙肢弱连梁”及连梁“强剪弱弯”的设计目标能够实现。

现有研究成果大部分集中于套筒灌浆饱满的钢筋连接性能及套筒灌浆饱满的装配式混凝土结构抗震性能,对于套筒灌浆缺陷的钢筋接头和结构研究较少。目前,李向民等^[25]开展了灌浆缺陷对钢筋套筒灌浆连接接头强度影响的试验研究,结果表明,只要套筒端头灌浆缺陷长度不超过套筒内一侧钢筋锚固长度的30%,其接头的对中单向拉伸强度就能符合要求。郑清林^[26]、Xiao^[27]等分别开展了套筒灌浆缺陷对装配式混凝土柱和剪力墙抗震性能影响的试验研究,结果表明,灌浆缺陷会导致试件承载力和延性性能变差。

本文设计7个钢筋套筒灌浆连接的装配式混凝土剪力墙进行低周反复加载试验,重点分析试件滞回曲线、承载力、变形、刚度退化、延性和耗能能力等抗震性能指标,以期丰富套筒灌浆缺陷对装配式混凝土剪力墙抗震性能影响研究,为套筒灌浆缺陷结构的性能评估和后续处理提供参考。

1 试 验

1.1 试件设计与制作

设计7个钢筋套筒灌浆连接的装配式混凝土剪力墙,试件由混凝土底座、混凝土墙身和墙顶加载梁组成。混凝土底座尺寸为1400 mm(宽)×600 mm(高)×2900 mm(长),混凝土墙身尺寸为200 mm(厚)×1800 mm(长)×2800 mm(高),加载梁的截面尺寸为400 mm(宽)×400 mm(高)×2200 mm(长),加载梁中心至墙底面的垂直距离 H 为3 m,墙剪跨比为1.67。试件立面尺寸如图1所示。试件底座单独浇筑,混凝土墙身与加载梁共同浇筑,剪力墙与底座结合面进行粗糙处理,构件达到设计强度后再进行装配和灌浆。试件均采用HRB400E钢筋,墙两端设置长400 mm的边缘约束构件,柱内配置6 Φ 16(6 Φ 16表示6根直径为16 mm的HRB400E钢筋,下同)竖向钢筋和 Φ 8@200 mm箍筋,墙竖向分布钢筋为8 Φ 10,墙底面以上600 mm范围为水平分布筋加密区,加密区水平分布筋为 Φ 8@150 mm,非加密区水平分布筋为 Φ 8@200 mm,试件拉筋直径6 mm,剪力墙试件配筋如图2所示。

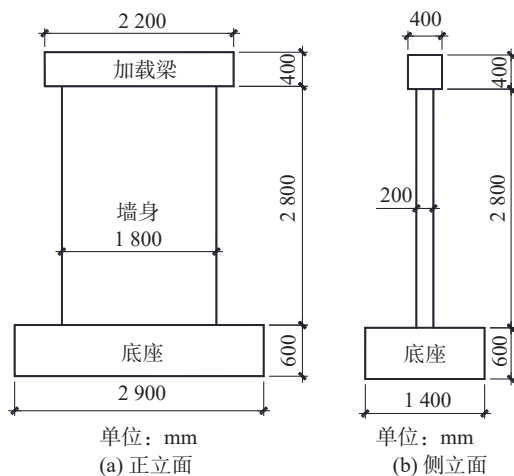
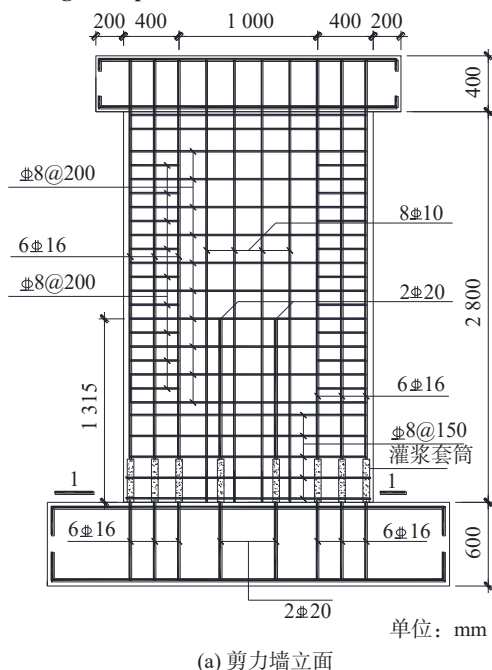
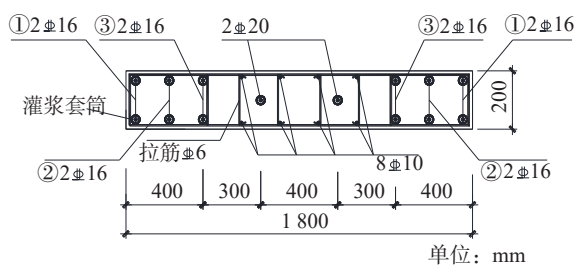


图1 剪力墙试件尺寸

Fig. 1 Specimen dimensions of shear wall



(a) 剪力墙立面



(b) 剪力墙1-1剖面

图2 剪力墙试件配筋

Fig. 2 Reinforcement of shear wall specimens

混凝土底座和墙身通过两端边缘构件12C16和中间部位2C20纵筋进行套筒灌浆连接,坐浆层厚度为20 mm。钢筋与灌浆料的设计锚固长度为8D(D为钢筋公称直径),通过在上侧钢筋表面设置不同长度的橡胶塞,可精确模拟套筒内灌浆缺陷,如图3所示。考虑套筒内上侧钢筋锚固长度小于5D时,钢筋灌浆套

筒连接件发生拔出破坏^[28],灌浆缺陷剪力墙的套筒内上侧钢筋与灌浆料锚固长度设置为 $4D$ 和 $5D$ 两种情况(即灌浆缺陷长度为 $4D$ 和 $3D$)。灌浆缺陷设置在剪力墙边缘构件的套筒内上侧钢筋锚固段,设置灌浆缺陷的套筒连接接头数量有4、8和12根3种情况。试件编号8D-BM表示试件全部套筒灌浆饱满;编号4D-QX1、5D-QX1分别表示试件①位置纵筋锚固长度为 $4D$ 和 $5D$;4D-QX2、5D-QX2分别表示试件①、②位置纵筋锚固长度为 $4D$ 和 $5D$;4D-QX3、5D-QX3分别表示试件①、②、③位置纵筋锚固长度均为 $4D$ 和 $5D$ 。试件①、②、③具体位置如图2(b)所示。试件设计参数详如表1所示。灌浆套筒尺寸如表2所示。

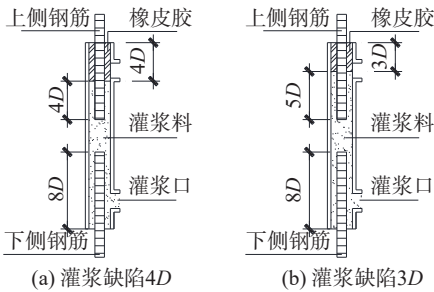


图3 套筒灌浆缺陷示意图

Fig. 3 Schematic diagram of grouting defects in the sleeves

表1 试件设计参数
Tab. 1 Design parameters of specimens

试件编号	N	L_a	L_0	L	$m/\%$
8D-BM	0	$8D$	0	0	0
4D-QX1	4	$4D$	$4D$	$16D$	16.7
4D-QX2	8	$4D$	$4D$	$32D$	33.3
4D-QX3	12	$4D$	$4D$	$48D$	50.0
5D-QX1	4	$5D$	$3D$	$12D$	12.5
5D-QX2	8	$5D$	$3D$	$24D$	25.0
5D-QX3	12	$5D$	$3D$	$36D$	37.5

注: N 为灌浆缺陷套筒的总数量; L_a 为套筒内上部钢筋的锚固长度; L_0 为套筒内灌浆缺陷长度; L 为整个试件的套筒灌浆缺陷总长; m 为整个试件的套筒灌浆缺陷率,本文 $m=L/96D$ 。

表2 灌浆套筒尺寸

Tab. 2 Geometry of grout sleeve

型号	全长	有效长度		外径	内径
		下段	上段		
GTZQ4-16	310	150	140	48	36
GTZQ4-20	370	180	170	52	40

1.2 材性性能

试件均采用同一批 $\Phi 40$ 商品混凝土,浇筑时预留3个标准混凝土立方体试块($150\text{ mm}\times 150\text{ mm}\times 150\text{ mm}$)。灌浆料采用高强无收缩灌浆料,灌浆时预留标准棱柱体试块($40\text{ mm}\times 40\text{ mm}\times 160\text{ mm}$)。试块与试件同条件

养护,28 d后进行抗压试验,混凝土立方体抗压强度实测值分别为45.82、45.92和47.94 MPa,立方体抗压强度平均值为46.56 MPa,灌浆料棱柱体抗压强度为95.4 MPa。

直径16 mm和20 mm的纵筋分别采用全灌浆GTZQ4-16和GTZQ4-20型套筒进行连接,灌浆套筒尺寸如表2所示。套筒采用球墨铸铁制作,抗拉强度 $\geq 550\text{ MPa}$,断后伸长率 $\geq 5\%$,球化率 $\geq 85\%$ 。依据标准试验方法对试验用钢筋进行材性测试,实测结果如表3所示。

表3 钢筋力学性能测试结果

Tab. 3 Material test results of reinforcements

钢筋直径/mm	屈服强度 f_y/MPa	抗拉强度 f_u/MPa	弹性模量 $E/(10^5\text{ MPa})$
8	467.68	648.36	2.06
10	453.21	652.63	2.05
16	441.81	655.57	2.03
20	470.26	633.54	1.96

1.3 试验加载制度及量测

试验加载装置如图4所示。试件设计轴压比为0.35^[29],首先在墙顶施加竖向压力至预定值,保持竖向压力不变,然后在墙顶施加水平往复力。竖向压力由加载梁顶部2 500 kN液压千斤顶提供,水平力由1 000 kN电液伺服作动器施加。试验采用位移控制的加载制度,试件屈服前每级位移增量为1 mm,循环1次;试件屈服后每级位移增量为4 mm,循环3次,当位移增加至40 mm后,每级位移增量调整为8 mm,再循环3次。当试件承载力下降到85%峰值荷载以下后停止加载。



图4 试验加载装置

Fig. 4 Loading device

分别在距离墙底150、1 400和2 650 mm的墙面布置位移计,以测量墙体不同高度处的位移变化。试验加载装置和位移测量布置如图5所示。对于套筒灌浆连接的纵筋,在距灌浆套筒顶端20 mm的上侧钢筋和距底座顶面20 mm的下侧钢筋处分别布置应变片,以测量纵向钢筋应变。应变片具体布置如图6所示。

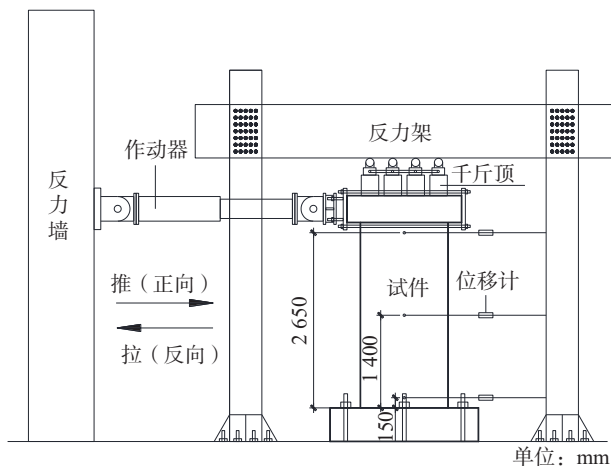


图5 加载装置和测量布置

Fig. 5 Test set-up and measurement arrangement

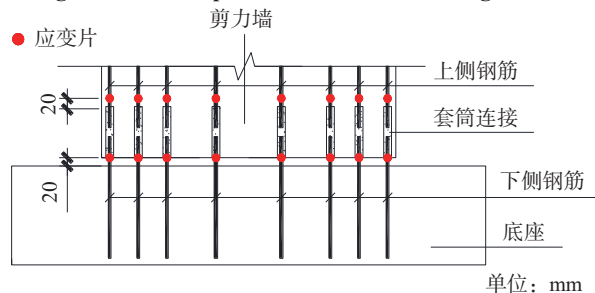


图6 应变片布置

Fig. 6 Location of strain gauges

2 试验结果及分析

2.1 破坏过程及试验现象

对于灌浆饱满试件8D-BM,水平位移为8 mm时,套筒顶部(距墙底高度约500 mm)开始出现水平裂缝。随着水平位移的增大,剪力墙底部以上1 000 mm的范围出现多条水平裂缝。水平位移为28 mm时,水平裂缝斜向下发展,大致呈45°;水平位移为36 mm时,墙体底部与坐浆层结合面出现水平裂缝,墙体角部出现竖向裂缝;水平位移为48 mm时,坐浆层处的水平裂缝贯通并发展为主要裂缝;水平位移为56 mm时,试件斜裂缝明显增多,墙底水平裂缝达4 mm;水平位移为64 mm时,墙体两侧角部套筒外侧以及套筒上方混凝土压碎(压碎部位高度约650 mm);水平位移为72 mm时,墙角套筒外层混凝土保护层整体脱落,套筒露出;水平位移为80 mm时,套筒发生倾斜,最外侧纵筋在套筒顶面上部拉断,承载力降至峰值的52%,试验结束。

对于灌浆缺陷试件4D-QX1、4D-QX2和4D-QX3,当水平位移分别为6、8和7 mm时,套筒顶部开始出现水平裂缝;当水平位移为28 mm时,水平裂缝开始斜向下约45°延伸;当水平位移为32 mm时,墙体底部与坐浆层结合面水平开裂,墙体角部出现竖

向裂缝;当水平位移为48 mm时,坐浆层处的水平裂缝贯穿,宽度达2 mm,逐渐发展成为主要裂缝;当水平位移为56 mm时,墙底主裂缝宽度增加,墙角竖向裂缝进一步增多;当水平位移为64 mm时,墙体两侧角部套筒外侧及套筒上方混凝土压碎(试件4D-QX1、4D-QX2和4D-QX3压碎部位高度分别约550、500和300 mm),墙底水平裂缝达5 mm;当水平位移为72 mm时,试件墙角套筒外层混凝土保护层整体脱落,套筒露出;当水平位移为80 mm时,试件4D-QX1和4D-QX2的套筒向平面外倾斜,最外侧纵筋在套筒顶面上部拉断,钢筋与灌浆料相对滑移较试件8D-BM严重,承载力分别降至峰值的79%和53%,试件4D-QX3承载力降至峰值的62%,试验结束。

对于灌浆缺陷试件5D-QX1、5D-QX2和5D-QX3,当水平位移分别为7、8和6 mm时,套筒顶部开始出现水平裂缝;当水平位移为28 mm时,水平裂缝开始呈45°斜向下发展;当水平位移为32 mm时,墙体底部与坐浆层结合面开裂,墙角出现竖向裂缝;当水平位移为56 mm时,墙底主裂缝宽度达5 mm;当水平位移为64 mm时,墙体两侧角部套筒外侧及套筒上方混凝土压碎(试件5D-QX1、5D-QX2和5D-QX3压碎部位高度分别约600、500和400 mm),试件5D-QX3套筒上方水平裂缝贯通,宽度达4 mm;当水平位移为72 mm时,墙角套筒外层混凝土保护层整体脱落,套筒露出;当水平位移为80 mm时,套筒向平面外倾斜,最外侧纵筋在套筒顶面上部拉断,钢筋与灌浆料相对滑移较试件8D-BM严重,试件5D-QX1、5D-QX2和5D-QX3的承载力分别降至峰值的43%、73%和76%,试验结束。

各试件破坏形态大致相同,均发生压弯破坏,最终破坏形态表现为边缘构件最外侧竖向钢筋受拉屈服甚至拉断,且墙角混凝土压碎剥落。与灌浆饱满试件相比,灌浆缺陷试件的水平裂缝稍微提前出现,主要由于上侧钢筋在套筒内的锚固长度减小,灌浆缺陷部位钢筋与套筒之间存在空隙,钢筋对套筒上部混凝土约束减弱。随着套筒内灌浆缺陷长度增加或墙内灌浆缺陷套筒数量由外侧向内侧增多,墙体角部套筒外侧及套筒上方混凝土压碎高度逐渐降低,原因可能是随着灌浆缺陷长度或灌浆缺陷套筒数量增加,上侧钢筋套筒连接部位整体耗能比例减小,相应高度处混凝土裂缝发展不充分。试件破坏阶段,墙角套筒外层混凝土保护层整体脱落,可见在工程设计中加强套筒周围水平钢筋的横向约束作用很有必要,可有效增强套筒与外侧混凝土保护层黏结性能。试件破坏后的形态及裂缝分布如图7所示。

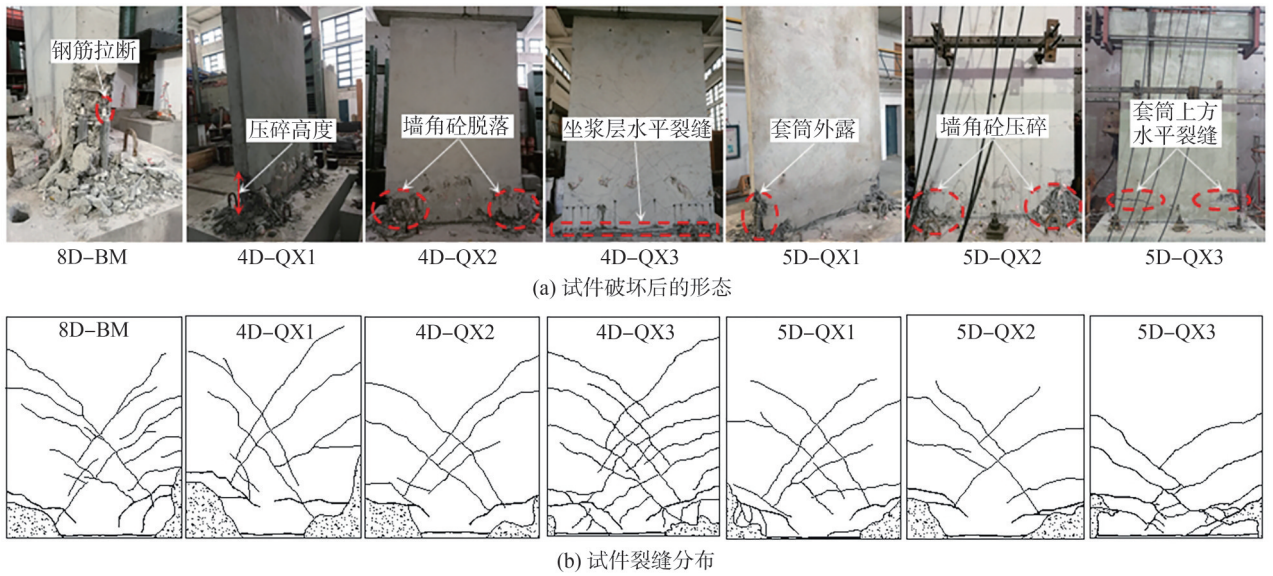


图7 试件破坏后的形态及裂缝分布

Fig. 7 Failure patterns and crack distribution of specimens after test

2.2 试件荷载-位移滞回曲线

实测试件的荷载 P -位移 Δ 滞回曲线如图8所示。

由图8可知,进入弹塑性受力阶段后,7个套筒灌浆连接装配式剪力墙的荷载-位移滞回曲线逐渐

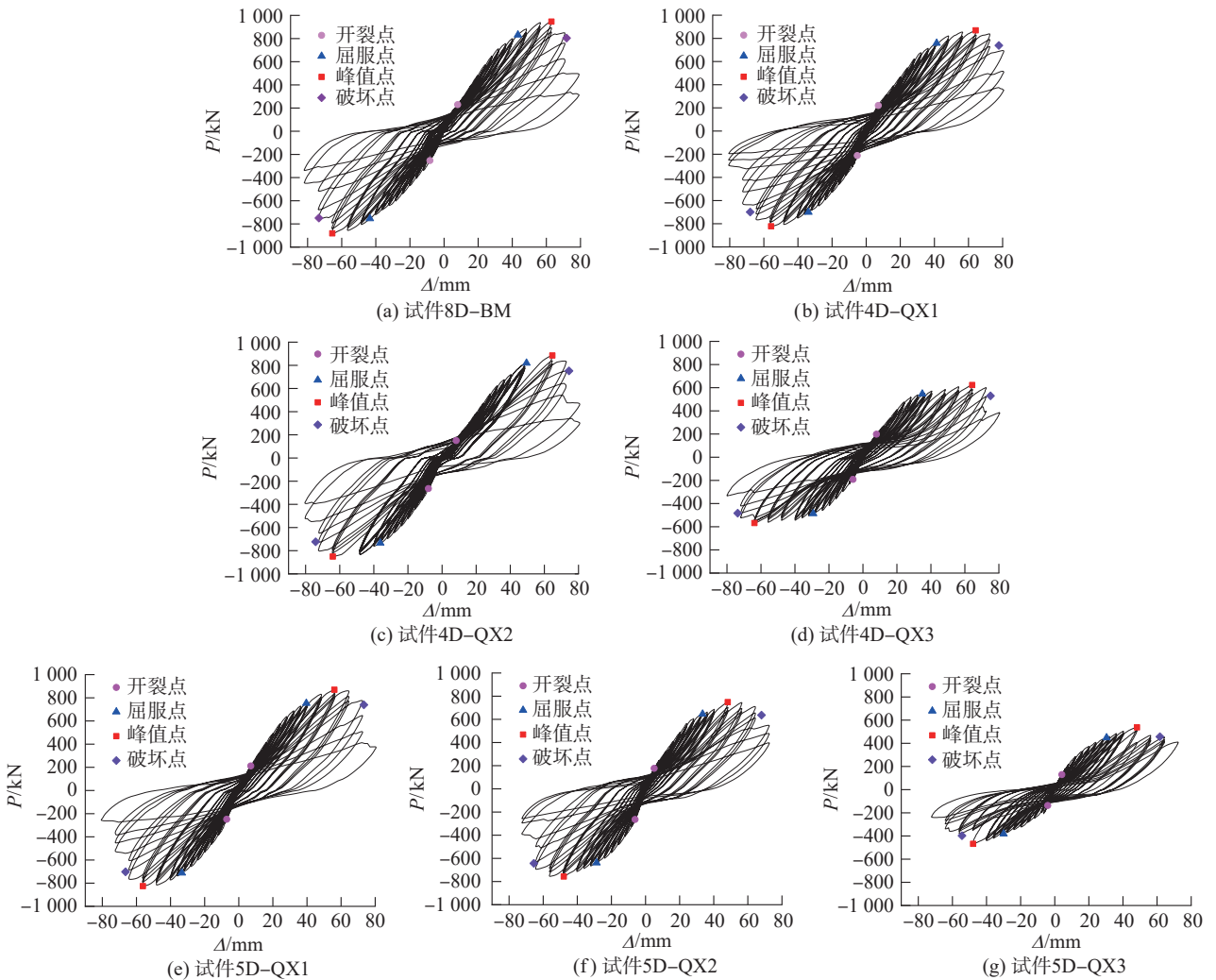


图8 试件荷载-位移滞回曲线

Fig. 8 Load-displacement specimens of hysteretic curves

呈弓形,随着位移的增大,试件滞回曲线逐渐转变成反“S”形。与灌浆饱满试件 8D-BM 相比,灌浆缺陷试件滞回曲线包围的面积相对较小;随着灌浆缺陷长度的增加,试件滞回曲线包围的面积相对减小,滞回曲线的峰值点变化不大,滞回曲线形状较为接近;随着边缘约束构件中灌浆缺陷套筒数量和套筒灌浆缺陷率增加,滞回曲线包围的面积明显减小,边缘约束构件中全部套筒设置灌浆缺陷(灌浆缺陷率达 50%)的试件滞回曲线的峰值点明显下降,抗震性能明显变差。

2.3 试件骨架曲线

各试件的荷载-位移骨架曲线如图 9 所示。由图 9 可知,套筒灌浆缺陷装配式混凝土剪力墙的荷载-位移骨架曲线可分为 3 个阶段:弹性段、弹塑性段和下降段。在加载初期,各试件曲线重合较好,灌浆缺陷对处于弹性阶段的装配式剪力墙受力性能影响较小。当骨架曲线进入非线性阶段后,不同灌浆缺陷试件骨架曲线上阶段斜率出现差异,与灌浆饱满试件 BM 相比,灌浆缺陷试件峰值承载力降低,其骨架曲线上阶段斜率变小,且随着灌浆缺陷套筒数量增加而趋于扁平状。当剪力墙顶点位移角 θ ($\theta=\Delta/H$) 达到大震作用下的弹塑性位移角限值 1/120,即试件水平位移为 25 mm 时,边缘构件局部套筒设置灌浆缺陷的试件承载力(取 4 个试件的均值)变化不大,减小约

1.4%,而边缘构件全部套筒设置灌浆缺陷的试件承载力(取 2 个试件的均值)降低幅值约为灌浆饱满试件的 25%。可见,与灌浆饱满试件相比,灌浆缺陷试件承载性能变差,且随着灌浆缺陷套筒数量的增大,试件受力性能劣化程度加剧。

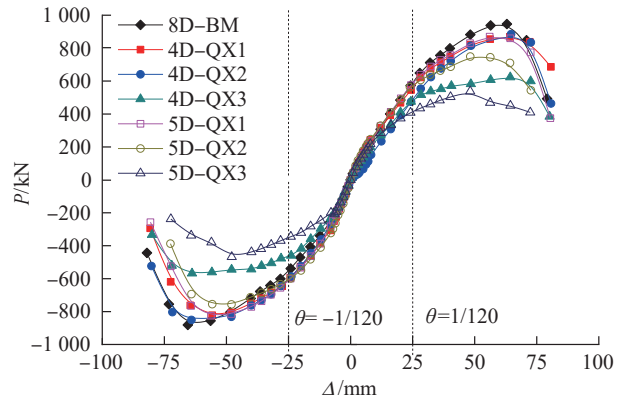


图 9 试件的荷载-位移骨架曲线

Fig. 9 Load-displacement specimens of skeleton curves

2.4 承载力

通过试验获取了受力破坏过程的开裂点、屈服点、峰值点和破坏点,具体数据如表 4 所示。表 4 中,开裂点对应试件首次出现裂缝时刻,屈服点采用等效能量法确定,峰值点为水平承载力最大值时刻,破坏点对应荷载-位移曲线下降到峰值承载力的 85% 时刻,为便于分析,数据取正负向的平均值。

表 4 试件特征点承载力及变形信息

Tab. 4 Bearing capacity and deformation of feature points of specimens

试件 编号	开裂点						屈服点					
	承载力/kN			位移/mm			承载力/kN			位移/mm		
	正向	负向	均值	正向	负向	均值	正向	负向	均值	正向	负向	均值
8D-BM	229.65	252.88	241.27	7.99	8.25	8.12	831.21	754.10	792.66	43.32	43.47	43.40
4D-QX1	220.74	211.40	216.07	7.12	5.23	6.18	758.32	700.51	729.42	41.33	33.84	37.58
4D-QX2	150.33	263.51	206.92	8.29	7.98	8.14	819.52	733.19	776.36	49.52	36.21	42.87
4D-QX3	198.67	191.29	194.98	7.96	5.83	6.90	546.60	486.50	516.55	34.97	29.26	32.11
5D-QX1	211.90	248.39	230.15	7.05	7.07	7.06	752.97	711.80	732.39	39.62	33.35	36.48
5D-QX2	176.89	264.05	220.47	5.07	6.11	5.59	646.35	638.71	642.53	33.47	28.73	31.10
5D-QX3	129.86	136.57	133.22	4.17	4.10	4.13	448.75	381.49	415.12	30.38	29.99	30.18

试件 编号	峰值点						破坏点						延性系数 μ		
	承载力/kN			位移/mm			承载力/kN			位移/mm					
	正向	负向	均值	正向	负向	均值	正向	负向	均值	正向	负向	均值	正向	负向	均值
8D-BM	946.35	881.22	913.79	62.98	65.54	64.26	804.40	749.04	776.72	71.88	73.36	72.62	1.66	1.69	1.67
4D-QX1	869.01	822.16	845.59	64.21	55.72	59.97	738.66	698.84	718.75	77.80	68.00	72.90	1.88	2.01	1.95
4D-QX2	884.73	850.57	867.65	64.68	64.06	64.37	752.02	722.98	737.50	74.44	74.16	74.30	1.50	2.05	1.78
4D-QX3	623.41	568.03	595.72	64.33	63.84	64.08	529.90	482.82	506.36	75.07	73.70	74.38	2.15	2.52	2.33
5D-QX1	869.77	825.61	847.69	56.06	56.22	56.14	739.30	701.77	720.54	73.36	66.40	69.88	1.85	1.99	1.92
5D-QX2	748.77	756.54	752.66	48.24	47.94	48.09	636.45	643.06	639.76	68.00	65.49	66.75	2.03	2.28	2.16
5D-QX3	537.84	467.81	502.83	48.22	47.86	48.04	457.16	397.64	427.40	61.67	54.38	58.03	2.03	1.81	1.92

图 10 为灌浆缺陷套筒数量对试件承载力的影响。由图 10 可见,随着套筒灌浆缺陷连接接头数量增多,试件特征点承载力逐渐降低。边缘构件全部套筒设置灌浆缺陷试件(QX3)的特征点承载力下降明显,其中,峰值承载力降低幅值约为灌浆饱满试件的 40%,边缘构件部分套筒设置灌浆缺陷试件的特征点承载力下降较小,峰值承载力降低幅值约为灌浆饱满试件的 9%。可见,当边缘约束构件全部套筒存在灌浆缺陷时,装配式混凝土剪力墙的承载能力退化严重,工程中此类灌浆缺陷结构后续补强处理措施尤为关键。

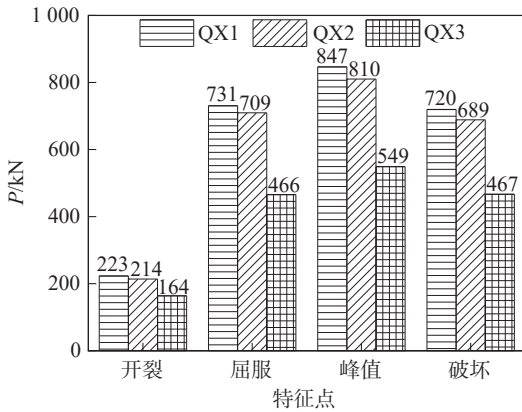


图 10 灌浆缺陷套筒数量对试件承载力的影响

Fig. 10 Effects of the number of defective grout sleeves on bearing capacity of specimens

灌浆缺陷长度对试件峰值承载力的影响如图 11 所示。由图 11 可知,套筒内上侧钢筋不同锚固长度(4D 和 5D)对峰值承载力的影响不大,原因是灌浆缺陷对试件承载力的影响与整个试件的套筒灌浆缺陷率有较大关系,试验中灌浆缺陷长度减小产生的灌浆缺陷率变化幅度不大(4.2%~12.5%),由于试验偶然因素的存在,部分上侧钢筋锚固长度为 5D 的试件(试件 5D-QX2 和试件 5D-QX3)与对应上侧钢筋锚固长度为 4D 的试件相比,峰值承载力反而更小。

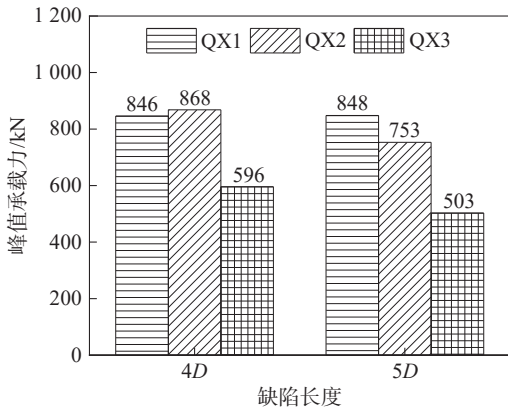


图 11 灌浆缺陷长度对试件峰值承载力的影响

Fig. 11 Effects of the length of grouting defects on peak bearing capacity of specimens

2.5 变形及延性

图 12 为灌浆饱满与灌浆缺陷试件的特征点位移对比。由图 12 可知,灌浆缺陷试件与灌浆饱满试件相比,开裂点位移下降了 22%,这是因为灌浆缺陷部位的套筒与内部纵筋之间存在空隙,导致套筒对混凝土纵向变形的约束力降低,开裂提前。灌浆缺陷试件屈服点位移下降了 19%,峰值点位移下降了 12%,灌浆缺陷试件破坏点位移下降不大,约为 4%。产生上述现象的原因可能是:一方面,由于灌浆缺陷的存在减少了灌浆料与钢筋之间的相互作用高度,钢筋套筒灌浆连接接头受拉变形性能变差,使得缺陷试件特征点水平位移变小;另一方面,灌浆缺陷的存在降低了钢筋和灌浆料之间的黏结性能,套筒内上部钢筋受拉滑移变形增大,使得缺陷试件特征点水平位移变大。两方面因素具有相互抵消作用,屈服点前荷载较小,上部钢筋滑移极小,使得试件屈服点位移下降较大(19%),荷载达到峰值点时,上部钢筋滑移有所增加,使得峰值点位移下降幅值变小(12%),峰值点后钢筋滑移变形加大,最终灌浆缺陷试件破坏点位移与饱满试件相比变化不大(4%)。

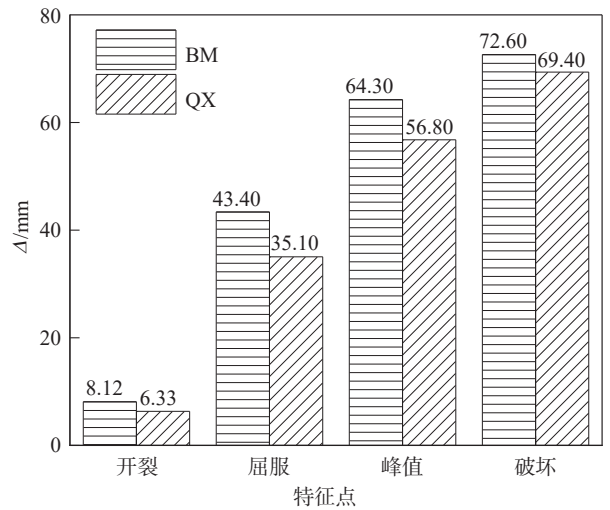


图 12 灌浆饱满与缺陷试件特征点位移对比

Fig. 12 Comparison between deformation of specimens with grouting defects and no defects

图 13 为灌浆缺陷套筒数量对试件位移的影响。由图 13 可知,随着套筒灌浆缺陷连接接头数量增多,试件特征点位移总体上逐渐减小,灌浆缺陷部位越多,试件整体变形性能越差。图 14 为灌浆缺陷长度对试件特征点位移的影响。由图 14 可知,当套筒内上侧钢筋锚固长度由 5D 减小至 4D 时,试件特征点位移变大,原因是当套筒内上侧钢筋锚固长度减小至 4D 时,钢筋与灌浆料之间提前发生黏结破坏,试件套筒内上侧钢筋受拉滑移变形增大。

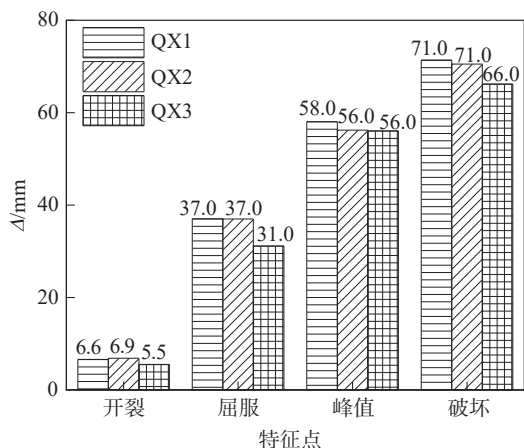


图 13 灌浆缺陷套筒数量对试件特征点位移的影响

Fig. 13 Effects of number of defective grout sleeves on deformation of feature points of specimens

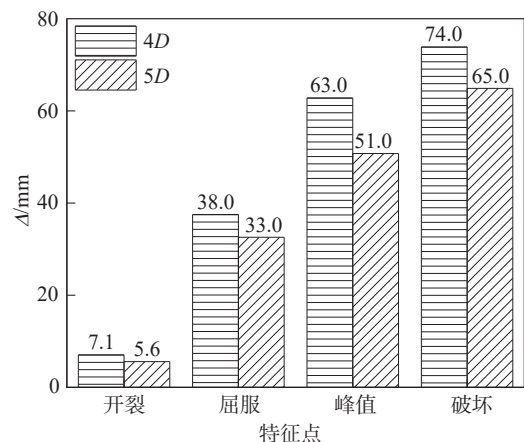


图 14 灌浆缺陷长度对试件特征点位移的影响

Fig. 14 Effects of length of grouting defects on deformation of feature points of specimens

试件延性采用破坏点位移 Δ_m 与屈服点位移 Δ_y 的比值进行衡量,即延性系数 $\mu=\Delta_m/\Delta_y$,各试件延性系数如表4所示。由表4可知,各试件的延性系数均小于3,灌浆缺陷试件的延性系数(取6个试件的均值)比灌浆饱满试件大,分别为2.01和1.67。主要原因在于灌浆缺陷的存在减小了试件的屈服点位移,试件屈服提前,但上侧钢筋与灌浆料的受拉滑移变形使得灌浆缺陷试件的破坏点位移变化很小,导致灌浆缺陷试件从屈服到破坏期间的延性性能相对较好。

2.6 刚度退化

以荷载-位移骨架曲线的割线刚度来探讨试件刚度退化过程,刚度值为:

$$K_i = \frac{|+P_i| + |-P_i|}{|+\Delta_i| + |-\Delta_i|} \quad (1)$$

式中, K_i 为刚度,是试件第*i*次循环的正负最大水平荷载 $+P_i$ 、 $-P_i$ 的绝对值之和与对应变形 $+\Delta_i$ 、 $-\Delta_i$ 绝对值之和的比值。

图15为试件刚度的退化曲线。由图15可知,试件

刚度随加载位移增大而逐渐减小,当加载控制位移较小时,套筒灌浆缺陷对刚度影响较小,随着位移的增大,灌浆缺陷试件刚度退化加快。边缘构件中所有套筒均设置灌浆缺陷的试件,其刚度退化明显比其他试件更快,在峰值荷载时,缺陷试件4D-QX3和5D-QX3的刚度仅为饱满试件8D-BM的65%和74%。可见,当边缘约束构件全部套筒存在灌浆缺陷时,装配式混凝土剪力墙抵抗变形的能力退化严重。

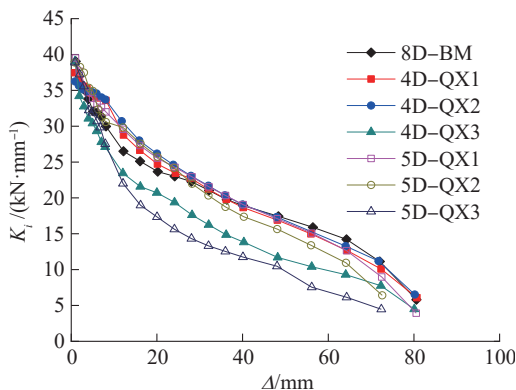


图 15 刚度退化曲线

Fig. 15 Stiffness degradation curves

试件特征点刚度如表5所示。由表5可知,灌浆缺陷试件刚度与灌浆饱满试件相比,开裂点刚度和屈服点刚度变化不大,峰值点刚度下降了8.5%,破坏点刚度下降了16.1%,原因是在灌浆缺陷高度范围内,钢筋与套筒不能通过灌浆料整体受力,套筒内钢筋屈服及滑移后,灌浆缺陷试件刚度受影响而加速退化。

表 5 试件不同特征点下的刚度

Tab. 5 Stiffness of different characteristic points

试件编号	开裂	屈服	峰值	破坏
8D-BM	29.71	18.27	14.22	10.70
4D-QX1	34.99	19.41	14.10	9.86
4D-QX2	25.44	18.11	13.48	9.93
4D-QX3	28.27	16.08	9.30	6.81
5D-QX1	32.60	20.07	15.10	10.31
5D-QX2	35.55	20.66	15.65	9.59
5D-QX3	32.22	13.75	10.47	7.37

图16为灌浆缺陷长度对试件刚度的影响。由图16可知,当套筒内上侧钢筋锚固长度减小,试件特征点刚度减小。图17为灌浆缺陷套筒数量对试件刚度的影响。由图17可知,随着套筒灌浆缺陷连接接头数量增多,试件特征点刚度逐渐减小,由于缺陷套筒数量增多产生的灌浆缺陷率变化幅度大于缺陷长度,缺陷套筒数量增加对试件刚度的影响大于缺陷长度,尤其是边缘约束构件中全部套筒设置灌浆缺陷的试件。

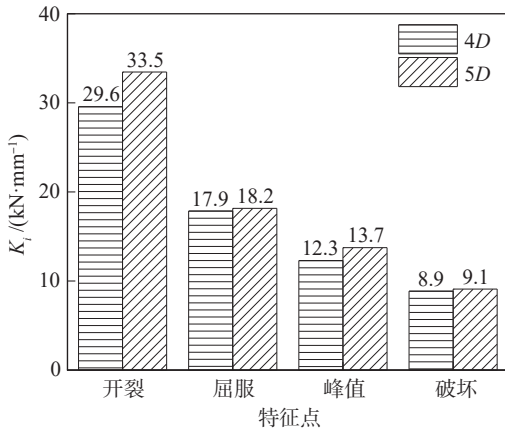


图 16 灌浆缺陷长度对试件特征点刚度的影响

Fig. 16 Effects of the length of grouting defects on stiffness of specimens

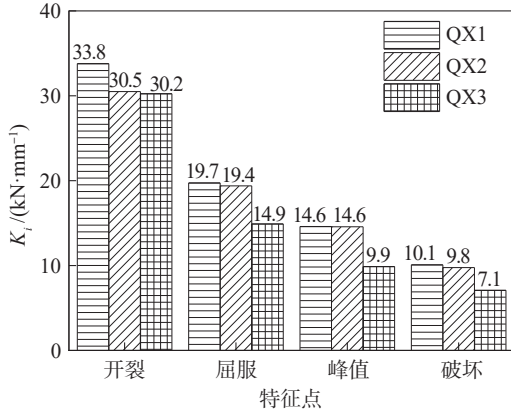


图 17 灌浆缺陷套筒数量对试件特征点刚度的影响

Fig. 17 Effects of number of defective grout sleeves on stiffness of feature points of specimens

2.7 耗能能力

用试验荷载-位移滞回环所包围的面积来衡量试件的能量耗散大小。图 18 为试件能量耗散大小随位移变化关系。由图 18 可知,随着水平位移的增大,试件能量耗散增加,峰值荷载后,试件能量耗散逐渐达到峰值,最后试件因套筒外侧混凝土严重脱落,能量耗散开始降低。表 6 给出了各试件特征点能量耗散大小。由表 6 可知:灌浆缺陷试件耗能与灌浆饱满试件相比,各特征点

表 7 试件不同控制位移的等效黏滞阻尼系数 h_e

Tab. 7 Equivalent damping coefficient of different displacement control of specimens

试件编号	控制位移/mm													
	8	12	16	20	24	28	32	36	40	48	56	64	72	80
8D-BM	0.04	0.05	0.04	0.04	0.03	0.03	0.04	0.04	0.04	0.06	0.07	0.08	0.11	0.17
4D-QX1	0.03	0.04	0.04	0.04	0.03	0.04	0.04	0.05	0.05	0.07	0.08	0.10	0.12	0.17
4D-QX2	0.04	0.04	0.04	0.03	0.03	0.03	0.03	0.04	0.04	0.06	0.08	0.08	0.11	0.19
4D-QX3	0.04	0.05	0.04	0.04	0.04	0.05	0.05	0.06	0.07	0.09	0.10	0.11	0.13	0.15
5D-QX1	0.03	0.04	0.04	0.03	0.03	0.04	0.04	0.05	0.05	0.07	0.09	0.10	0.14	0.22
5D-QX2	0.04	0.04	0.04	0.04	0.04	0.04	0.05	0.06	0.06	0.08	0.10	0.11	0.17	—
5D-QX3	0.04	0.05	0.05	0.06	0.06	0.07	0.07	0.08	0.08	0.10	0.11	0.11	0.11	—

能量耗散均减小;随着套筒灌浆缺陷连接接头数量和灌浆缺陷长度增加,试件各特征点能量耗散均减小。

试件的耗能能力用等效黏滞阻尼系数 h_e (表 7) 来衡量。图 19 为黏滞阻尼系数与水平位移关系。由图 19 可知,在试件屈服点位移以前,试件耗能系数变化不大, h_e 约为 0.05,但峰值点位移后,试件耗能系数显著增大,当水平位移为 80 mm 时, h_e 达到了 0.18 左右。试件 QX1、QX2 和 QX3 的最大等效黏滞阻尼系数分别为 0.20、0.19 和 0.15,随着套筒灌浆缺陷连接接头数量增多,阻尼系数减小,试件耗能能力变差,缺陷套筒数量增加对试件等效阻尼系数的影响大于缺陷长度。

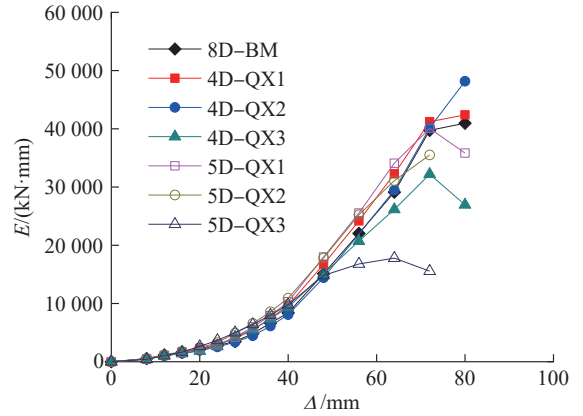


图 18 能量耗散和水平位移的关系

Fig. 18 Relationship between energy consumption and horizontal displacements

表 6 试件不同特征点的能量耗散

Tab. 6 Energy consumption of specimens of different characteristic points

试件编号	kN·mm			
	开裂	屈服	峰值	破坏
8D-BM	560	11 240	29 366	39 810
4D-QX1	369	8 337	28 195	41 345
4D-QX2	433	10 195	29 805	42 550
4D-QX3	431	5 628	26 194	30 653
5D-QX1	475	8 215	25 645	38 464
5D-QX2	488	6 180	17 856	32 640
5D-QX3	265	5 805	14 810	17 055

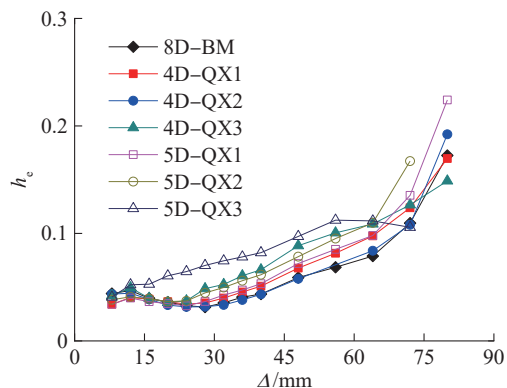


图19 等效黏滞阻尼系数与水平位移关系

Fig. 19 Relationship between equivalent damping coefficients and horizontal displacements

3 结论

通过6个存在灌浆缺陷的钢筋套筒灌浆连接装配式足尺剪力墙试件和1个套筒灌浆饱满对比试件的拟静力试验,深入分析了灌浆缺陷对装配式足尺混凝土剪力墙抗震性能的影响,得到以下主要结论。

1)套筒灌浆缺陷装配式剪力墙的破坏形态与灌浆饱满装配式剪力墙的相似,均发生压弯破坏,最终破坏形态表现为边缘构件最外侧竖向钢筋受拉屈服甚至因套筒倾斜而拉断,且墙角套筒外层混凝土保护层层压碎脱落。

2)套筒灌浆缺陷装配式剪力墙的荷载-位移滞回曲线呈弓形或反“S”形,随着灌浆缺陷长度和缺陷套筒数量增多,套筒灌浆缺陷率增加,滞回曲线包围的面积减小,抗震性能变差。

3)灌浆缺陷对试件初始刚度影响不明显,但对后期峰值点和破坏点刚度的影响逐渐变大,试件刚度随着灌浆缺陷套筒数量和套筒内灌浆缺陷长度增加而减小,试验中缺陷套筒数量增加产生的灌浆缺陷率变化幅度大,其对试件刚度的影响大于缺陷长度。

4)试件承载力和变形受灌浆缺陷影响而减小,承载力随着灌浆缺陷套筒数量和灌浆缺陷长度增加而减小,缺陷套筒数量增加对试件承载力的影响大于缺陷长度。特征点位移随着灌浆缺陷套筒数量增多而减小,随着灌浆缺陷长度增加而增大。

5)试件能量耗散能力受灌浆缺陷影响而变差,随着灌浆缺陷套筒数量和灌浆缺陷长度增加,阻尼系数减小,抗震耗能能力变差,缺陷套筒数量增加对试件耗能能力的影响大于缺陷长度。

参考文献:

[1] Xue Weichen, Huang Qian, Yang Jialin, et al. Cyclic response of precast concrete shear walls with reduced grouted sleeves or corrugated metallic duct splices[J]. Case Studies in Con-

struction Materials, 2023, 18: e01822.

- [2] Wang Kun, Liu Wenguang, Yang Sen, et al. Seismic behavior of a hollow precast concrete shear wall with insulation under high axial compression ratios[J]. Engineering Structures, 2024, 318: 118672.
- [3] Vieira D R, Calmon J L, Coelho F Z. Life cycle assessment (LCA) applied to the manufacturing of common and ecological concrete: A review[J]. Construction and Building Materials, 2016, 124: 656-666.
- [4] Liang Zihao, Gong Chao, Hu Yi, et al. Effects of different horizontal joints on seismic performance of precast shear walls[J]. Journal of Building Structures, 2024, 45(Supp1): 216-227. [梁梓豪, 龚超, 胡义, 等. 水平接缝连接对装配式混凝土剪力墙抗震性能的影响[J]. 建筑结构学报, 2024, 45(增刊1): 216-227.]
- [5] Zhang Shiqian, Chen Yueshi, Liu Yanan, et al. State of the art in connection of vertically distributed reinforcements for precast shear wall[J]. Journal of Southwest Jiaotong University, 2021, 56(4): 828-838. [张士前, 陈越时, 刘亚男, 等. 装配式剪力墙竖向分布钢筋连接程度研究进展[J]. 西南交通大学学报, 2021, 56(4): 828-838.]
- [6] Li Ran, Huang Xiaokun, Tian Chunyu. Comparative study on mechanical properties of three kinds of assembled monolithic reinforced concrete shear wall structures[J]. Journal of Building Structures, 2018, 39(Supp2): 79-85. [李然, 黄小坤, 田春雨. 三种装配整体式钢筋混凝土剪力墙结构受力性能对比研究[J]. 建筑结构学报, 2018, 39(增刊2): 79-85.]
- [7] Zhu Zhangfeng, Guo Zhengxing, Tang Lei. Experimental study and FEA on seismic performance of new hybrid precast concrete shear walls[J]. China Civil Engineering Journal, 2018, 51(3): 36-43. [朱张峰, 郭正兴, 汤磊. 新型混合装配式混凝土剪力墙抗震性能试验研究及有限元分析[J]. 土木工程学报, 2018, 51(3): 36-43.]
- [8] Tang Hongyuan, Tan Hongfei, Zhang Jinfang, et al. Study on seismic behavior of prefabricated shear wall with pressed cone sleeves(PCSs)[J]. Soil Dynamics and Earthquake Engineering, 2024, 184: 108824.
- [9] Xue Weichen, Hu Xiang. State of the art of studies on precast concrete shear wall structures[J]. Journal of Building Structures, 2019, 40(2): 44-55. [薛伟辰, 胡翔. 预制混凝土剪力墙结构体系研究进展[J]. 建筑结构学报, 2019, 40(2): 44-55.]
- [10] Gu Sheng, Gu Jimben, Guo Junyuan, et al. Seismic performance of precast concrete shear wall with treatments of connecting reinforcement defects in grouted sleeves under combined axial tension and cyclic horizontal load[J]. Journal of Building Engineering, 2024, 97: 110941.
- [11] Xie Linlin, Liu Qiang, Wang Xinyu, et al. Experimental study on seismic performance of precast concrete shear walls with defective and repaired grouted sleeve[J]. Structures, 2023, 57: 105071.
- [12] Wang Xinyu, Xie Linlin, Liu Qianmin. Full-scale experimental study on seismic performance of repaired precast shear walls[J]. Soil Dynamics and Earthquake Engineering, 2023, 175: 108225.
- [13] Seo S Y, Nam B R, Kim S K. Tensile strength of the grout-filled head-splice-sleeve[J]. Construction and Building Ma-

- terials,2016,124:155–166.
- [14] Henin E, Morcoux G. Non-proprietary bar splice sleeve for precast concrete construction[J]. *Engineering Structures*, 2015, 83:154–162.
- [15] Ling J H, Rahman A B A, Ibrahim I S. Feasibility study of grouted splice connector under tensile load[J]. *Construction and Building Materials*, 2014, 50:530–539.
- [16] Ling J H, Rahman A B A, Ibrahim I S, et al. Behaviour of grouted pipe splice under incremental tensile load[J]. *Construction and Building Materials*, 2012, 33:90–98.
- [17] Yu Qiong, Sun Jiaqiu, Yuan Weihang. Experimental study on bond behavior between ribbed steel bars and sleeve constrained grouting material[J]. *Journal of Harbin Institute of Technology*, 2018, 50(12):98–106. [余琼, 孙佳秋, 袁炜航. 带肋钢筋与套筒约束灌浆料黏结性能试验[J]. 哈尔滨工业大学学报, 2018, 50(12):98–106.]
- [18] Xu Chengshun, Liu Hongtao, Du Xiuli. Experimental study on connection performance of grouted sleeve splicing for rebars under high stress repeated tension-compression loading [J]. *Journal of Building Structures*, 2018, 39(12):178–184. [许成顺, 刘洪涛, 杜修力. 高应力反复拉压作用下钢筋套筒灌浆连接性能试验研究[J]. 建筑结构学报, 2018, 39(12):178–184.]
- [19] Zheng Yongfeng, Guo Zhengxing, Zhang Xin. Effect of sleeve inner cavity structure on bond performance of grouted pipe splice[J]. *Journal of Building Structures*, 2018, 39(9):158–166. [郑永峰, 郭正兴, 张新. 套筒内腔构造对钢筋套筒灌浆连接黏结性能的影响[J]. 建筑结构学报, 2018, 39(9):158–166.]
- [20] Li Rui, Zheng Yimin, Zhao Yong. Experimental research on seismic performance of precast concrete columns with 500 MPa reinforcements splicing by grout-filled coupling sleeves[J]. *Journal of Building Structures*, 2016, 37(5):255–263. [李锐, 郑毅敏, 赵勇. 配置 500 MPa 钢筋套筒灌浆连接预制混凝土柱抗震性能试验研究[J]. 建筑结构学报, 2016, 37(5):255–263.]
- [21] Yu Qiong, Sun Jiaqiu, Xu Xuejing, et al. Experimental study on seismic behavior of precast shear walls with reinforcement spliced by grouted sleeve lapping connector[J]. *Journal of Tongji University(Natural Science)*, 2018, 46(10):1348–1359. [余琼, 孙佳秋, 许雪静, 等. 钢筋套筒灌浆搭接连接的预制剪力墙抗震试验[J]. 同济大学学报(自然科学版), 2018, 46(10):1348–1359.]
- [22] Ma Junwei, Pan Jinlong, Yin Wanyun, et al. Experimental study on seismic behavior of wholly precast RC frame-shear wall structure[J]. *Journal of Building Structures*, 2017, 38(6):12–22. [马军卫, 潘金龙, 尹万云, 等. 全装配式钢筋混凝土框架-剪力墙结构抗震性能试验研究[J]. 建筑结构学报, 2017, 38(6):12–22.]
- [23] Liu Hongtao, Yan Qiushi, Du Xiuli. Study of seismic performance of reinforced concrete frame beam-column joints connected with grouted sleeves[J]. *Journal of Building Structures*, 2017, 38(9):54–61. [刘洪涛, 闫秋实, 杜修力. 钢筋混凝土框架梁柱节点灌浆套筒连接抗震性能研究[J]. 建筑结构学报, 2017, 38(9):54–61.]
- [24] Qian Jiaru, Han Wenlong, Zhao Zuozhou, et al. Pseudo-dynamic substructure test on a 3-story full-scale model of prefabricated concrete shear wall structure with rebars splicing by grout sleeves[J]. *Journal of Building Structures*, 2017, 38(3):26–38. [钱稼茹, 韩文龙, 赵作周, 等. 钢筋套筒灌浆连接装配式剪力墙结构三层足尺模型子结构拟动力试验[J]. 建筑结构学报, 2017, 38(3):26–38.]
- [25] Li Xiangmin, Gao Rundong, Xu Qingfeng, et al. Experimental study on influence of grouting defect on joint strength of grout sleeve splicing of rebars[J]. *Building Structure*, 2018, 48(7):52–56. [李向民, 高润东, 许清风, 等. 灌浆缺陷对钢筋套筒灌浆连接接头强度影响的试验研究[J]. 建筑结构, 2018, 48(7):52–56.]
- [26] Zheng Qinglin, Wang Ni, Tao Li, et al. Experimental study on effects of grout defects on seismic performance of assembled concrete columns[J]. *China Civil Engineering Journal*, 2018, 51(5):75–83. [郑清林, 王霓, 陶里, 等. 套筒灌浆缺陷对装配式混凝土柱抗震性能影响的试验研究[J]. 土木工程学报, 2018, 51(5):75–83.]
- [27] Xiao Shun, Wang Zhuolin, Li Xiangmin, et al. Study of effects of sleeve grouting defects on the seismic performance of precast concrete shear walls[J]. *Engineering Structures*, 2021, 236:111833.
- [28] Zheng Guanyu, Kuang Zhiping, Xiao Jianzhuang, et al. Mechanical performance for defective and repaired grouted sleeve connections under uniaxial and cyclic loadings[J]. *Construction and Building Materials*, 2020, 233:117233.
- [29] 中华人民共和国住房和城乡建设部. 高层建筑混凝土结构技术规程:JGJ3—2010[S]. 北京:中国建筑工业出版社, 2010.

Effects of Grout Defects on Seismic Behavior of Precast Concrete Shear Wall

ZHENG Wei, ZHANG Shiqian, MA Minglei, YIN Guanghua, CHEN Shaojun

(China Construction Eighth Engineering Division Company Limited, Shanghai 200122, China)

Abstract:

Objective Precast concrete structure has obvious advantages such as improving production efficiency, saving energy and green environmental protection. Precast concrete shear wall is widely used in high-rise residential buildings, which plays an important role in promoting the industrialization of housing. The reliability of the vertical connection of precast concrete shear walls is very important to ensure the mechanical performance of the structural system. The seismic behavior of precast concrete shear wall with grout defects were analyzed. This paper study the effect of sleeve grouting defects on the seismic performance of precast concrete shear wall, and provides a reference for the performance evaluation and subsequent treatment of sleeve grouting defects.

Methods Seven prefabricated concrete shear walls (six test specimens with grouting defects and one test specimen with full grouting) connected by reinforcement sleeve grouting were designed for low cycle repeated loading tests. The main designed parameters of the specimens in the tests

were the number of sleeves with grouting defects and the length of grouting defects that reduced the anchorage lengths between upper reinforcements and grout. The design anchorage length of reinforcement bar and grout material was $8D$ (D is the nominal diameter of reinforcement bar). By setting rubber plugs of different lengths outside the upper reinforcement bar, the grout defects in the sleeve were accurately simulated. The anchorage length of upper reinforcement bar and grout material in the sleeve of specimens was $4D$ and $5D$. The grouting defect was set in the sleeve of the edge members of shear wall. The number of sleeve joints with grouting defect is 4, 8 and 12 in three cases. The design axial compression ratio of the specimens was 0.35. First, vertical pressure was applied to the top of the wall to a predetermined value, keeping the vertical pressure unchanged, and then horizontal reciprocating force was applied to the top of the wall. The vertical pressure was provided by hydraulic jack at the top of loading beam, and horizontal force was applied by the electro-hydraulic servo actuator. The loading system of displacement control was adopted in the test. The failure process and final failure mode were observed. The hysteretic curves of horizontal force-displacement were obtained. The hysteresis loops, bearing capacity, deformation, stiffness degradation, ductility and energy dissipation capacity of specimens were analyzed.

Results and Discussions The test results indicated that the failure mode of precast concrete shear wall with grouting defects was the same as that of the specimen with no defects. The final failure modes of walls could be characterized as the outside longitudinal reinforcements of edge members yielded even broke because of inclined sleeve, and concrete cover outside the sleeve crushed and peeled in the corner of wall. Compared with full grouting specimen, the horizontal crack of grouting defect specimen appeared slightly earlier. As the number of grouting defect sleeves in the wall increased, crushing height of concrete outside corner sleeve decreased gradually. The hysteretic curves of load-displacement of specimens with grouting defects look like bow or reversed S-shape, and the pinching effect of curves showed more obvious with the increase of the number of defective grout sleeves. The load-displacement skeleton curve of precast concrete shear wall with sleeve grouting defects was divided into three stages: elastic section, elastoplastic section and falling section. At the initial stage of loading, the curves of the specimens had good coincidence, and the grouting defects had little influence on the mechanical performance of the precast shear wall in elastic stage. When the skeleton curve entered the nonlinear stage, the slope of the upward section of the skeleton curve of different grouting defect specimens was different. Compared with full grouting specimen, the peak bearing capacity of grouting defect specimens decreased, the slope of the upward section of the skeleton curve became smaller, and tended to be flat with the increase of grouting defect sleeves. With the increase of number of sleeve grouting defects, the bearing capacity of specimens gradually decreased. The bearing capacity of specimen with all grouting defect sleeves of edge member decreased obviously, and the peak bearing capacity decreased by about 40% of full grouting specimen. The influence of different grouting defect lengths on the peak bearing capacity was not significant. Compared with full grouting specimen, the displacement at crack point, yield point and peak point of grouting defect specimens decreased more, but the displacements at failure point decreased less. With the increase of sleeve grouting defects, the displacement of feature points gradually decreased, and the more grouting defects, the worse the overall deformation performance of specimen. The ductility coefficient of all specimens was less than 3, and the ductility coefficient of grouting defect specimen was larger than that of grouting full specimen. The stiffness of specimen decreased gradually with the increase of loading displacement. When the displacement was small, the grouting defect has little influence on the stiffness. With the increase of displacement, the stiffness degradation of the grouting defect specimen accelerates. The stiffness degradation of specimen with grouting defects in all the sleeves of edge members was significantly faster than that of other specimens. Compared with grouting specimen, the energy dissipation of grouting defect specimen reduced. Before the yield displacement of specimen, the energy dissipation coefficient changed little. With the increase sleeve grouting defects, the energy dissipation of specimen decreased.

Conclusions The failure mode of precast concrete shear wall with grouting defects was the same as that of specimen with no defects. The hysteretic curves of load-displacement with grouting defects look like bow or reversed S-shape, and the pinching effect of curves showed more obvious with the increase of the number of defective grout sleeves. The bearing capacity, deformation and energy dissipation capacity reduced with the effects of grout defects, while the effect of grout defects on initial stiffness was slight. The bearing capacity, peak deformation and energy dissipation capacity reduced with the increase of the number of defective grout sleeves. The stiffness reduced with the increase of the number of defective grout sleeves and the length of grouting defects.

Key words: precast shear wall; grout sleeve splicing; grout defects; seismic behavior; quasi-static tests

(编辑 周 璇)

引用格式: Zheng Wei,Zhang Shiqian, Ma Minglei, et al. Effects of grout defects on seismic behavior of precast concrete shear wall[J]. *Advanced Engineering Sciences*, 2025, 57(5): 52-63. [郑巍, 张士前, 马明磊, 等. 套筒灌浆缺陷对装配式剪力墙抗震性能的影响[J]. *工程科学与技术*, 2025, 57(5): 52-63.]